Advances in Science and Technology Research Journal

Advances in Science and Technology Research Journal 2023, 17(5), 208–219
https://doi.org/10.12913/22998624/172406
ISSN 2299-8624, License CC-BY 4.0

Received: 2023.08.28
Accepted: 2023.09.15
Published: 2023.10.20

Multi-Variant Analysis of the Cross Wedge Rolling Process for Producing Railcar Axles

Zbigniew Pater[1], Janusz Tomczak[1], Tomasz Bulzak[1*]

[1] Lublin University of Technology, ul. Nadbystrzycka 36, 20-618 Lublin, Poland

* Corresponding author's e-mail: t.bulzak@pollub.pl

ABSTRACT

This study investigates the cross wedge rolling (CWR) process for manufacturing a rail axle in a scale of 1:6. Three cases of the rolling process are modelled numerically: standard rolling, wasteless rolling and rolling from a preform. The rolling cases under analysis are compared in terms of material and energy consumption, forming loads as well as propensity to internal and external defect formation. Using the Cockcroft-Latham criterion and the limits of this criterion determined by the rotary compression test, an assessment was made of the propensity of the material to fracture during the rolling processes analysed. Based on numerical results, standard CWR is selected for experimental verification. Obtained experimental results confirm that CWR is an effective method for producing railcar axles that are free from both internal and external defects. The experimental and numerical results obtained confirm that cross wedge rolling technology can be successfully used under industrial conditions for the production of long axles or shafts.

Keywords: cross-wedge rolling, railcar axle, FEM, experiment.

INTRODUCTION

Cross wedge rolling (CWR) is an advanced technique for manufacturing axisymmetric parts such as stepped axles and shafts [1]. Development work on cross wedge rolling technology focuses on: elimination of cracking of the rolled part, minimisation of material and energy consumption. In cross wedge rolling it is possible to produce parts with significantly lower forming forces than in other forming processes such as drop forging or extrusion. Lower forming forces result from the incremental shaping of parts during cross wedge rolling. In the entire production cycle with cross wedge rolling technology, approximately 90 % of the energy consumed is required to heat the material to the hot forming temperature [2]. Reduced rolling forces translate into less tool wear and less elastic deformation of the machine body (higher forging accuracy). Material cracking in cross wedge rolling processes is caused by the Mannesmann effect. The Mannesmann effect is caused by the alternating compression and tension of the rolled material [3]. Changes in the nature of the stresses and the complex state of deformation lead to a breach in the cohesion of the material. The main objective of research related to material cracking in the CWR process is to minimise this phenomenon and to be able to predict it using FEM [4, 5]. The main advantage of CWR is reduced material consumption compared to an alternative way of fabricating such parts, i.e. die forging. Material losses in CWR are generally below 10% and result from the necessity of cutting off defective workpiece ends with concavities that are formed because the material flows on the surface [6].

With a view to reducing material consumption in CWR, numerous research centre have undertaken research on developing methods for preventing the formation of concavities or at least reducing their size. Guo and Lu [7] investigated the effect of the basic parameters of CWR (forming angle α, wedge angle β and area reduction ΔA) on the cut-off material volume. The results showed

that the volume did not depend on the α angle but would decrease with increasing the β angle and increase with increasing the area reduction ΔA. Similar observations were made in a numerical analysis by Sun et al. [8], who stated that an increase in the β angle would lead to a decrease in the concavity depth *h*, while an increase in the area reduction Δ*A* would cause an increase in *h*. Pater et al. [9] analysed 21 cases of rolling and found that the concavity depth *h* was more likely to be higher if greater reduction ratios δ (where $\delta=d_0/d$; d_0 – billet initial diameter, d – diameter after rolling) and higher rolling speeds were used; it was also found that the concavity depth *h* could be decreased by using wedge tools with a greater value of the product and by increasing the forming temperature *T*. The numerical results were used to establish a formula for calculating end waste material allowance.

Previous studies have investigated three methods for decreasing concavity depth on the ends of a workpiece in order to reduce the volume of waste material. The first method was to constrain metal flow in the axial direction by means of side guides. This solution was described in studies by Shu et al. [10] and Pater et al. [11]. The second method involved providing the tool with a specially designed wedge block. The wedge block would constrain a certain volume of material at the end of the billet first and then would shape it into a taper. This method was described in studies by Wei et al. [12] and Shu et al. [13]. Shortcomings of this solution include a relatively high length of the wedge block as well as the possibility of overlap formation. The third method of end waste elimination was to use profiled billets with tapered and circular-arc ends [14, 15], as well as variable cone angle ends [16]. The profiled ends would be shaped in a separate operation which, in some cases (tapered ends), could be combined with roll cutting a bar into a conical end blank. An example of this solution was proposed by Wang et al. [17].

The problem of side waste material reduction becomes significant when it comes to rolling large parts that are manufactured in large lots. Such products include railcar axles with their weight even exceeding 400 kg. Railcar axes are produced by cogging and swaging methods [18]. Studies are currently conducted on making the CWR process suitable for manufacturing railcar axles. The primary limitation of using CWR in the production of railcar axles is connected with the large size of these parts and hence the need for tools with large overall dimensions. A recent study conducted by Pater [19] showed that the standard CWR process for manufacturing railway axles could be conducted using a rolling mill with rolls that had a nominal diameter of 1800 mm. However, the problem is that there exist no rolling mills that would be equipped with the rolls of such dimensions. In light of the above, numerous studies (e.g. by Sun et al. [20], Peng et al. [21], Bulzak [22]) recommended using multi-wedge synchrostep cross wedge rolling in which a railcar axle would be rolled by several wedges simultaneously.

The objective of this study is to investigate how end waste material could be eliminated in CWR of railcar axles and tool length could be reduced thereby. Given the wide range of the analysed samples of the CWR process, this study focuses primarily on numerical modelling. Only one of the analysed cases of CWR is investigated experimentally.

METHODOLOGY

The FE analysis was made using the Forge® program which had been effectively used in previous studies to simulate CWR processes. In 2005 Piedrahita et al. [23] used numerical modelling to determine the effect of the basic parameters of CWR on the occurrence of failure modes such as slip and necking. Silva et al. [24] modelled the mechanism of fracture in the axial zone of the workpiece. The fracture was induced by deleting elements in which the damage function exceeded the critical value. Studies [25-28] investigated the cross wedge rolling process of preforms for crankshafts. A similar study was conducted by Perez and Ambrosio [29], who developed a forging process for producing a stepped shaft from a rolled preform. Gutierez et al. [30] investigated the tool life in CWR of preforms for connecting rods. Pater and Tomczak [31] investigated the CWR process of a stepped shaft for gearboxes that was conducted in a two-roll mill. Pater et al. [32] used Forge® to develop innovative CWR methods for producing grinding media balls. This program was also used to investigate new solutions for rolling large-size parts such as railcar axles [19, 33, 34]. Kruse et al. [35] investigated the cross wedge rolling of serially arranged hybrid parts made of aluminium alloy and steel. Pater et al. [36] developed a new test for damage function calibration based on CWR. Summarizing the above, it should be emphasized that the

numerical models used in these studies have been experimentally verified, and the experimental results obtained have confirmed that Forge® is an effective tool for analyzing the CWR process.

Figure 1 shows the railcar axle rolled in a scale of 1:6 which is the object of analysis in this paper. This axle has one largest diameter region at the centre and two identical smaller diameter regions on its ends. Assuming that rolling would be carried out from a workpiece with its initial diameter equal to the largest diameter at the workpiece centre, it was possible to calculate the maximum area reduction ΔA, which amounted to 58.5%. This reduction value occurs when the lower diameter regions are deformed on the workpiece ends, as the conditions occurring in this stage of the rolling process are conducive to their formation.

CWR was assumed to be performed using flat wedges (Fig. 2), only one of which (upper wedge) would be moving in a linear fashion with a speed of 300 mm/s. The adopted rolling scheme and the scale (1:6) of a produced axle were determined by the lab conditions at the Lublin University of Technology. The study investigated three example of CWR, each realised with the use of tools of different design. The three rolling processes were conducted according to the schemes shown in Figure 2 and were denoted as i) standard rolling, ii) wasteless rolling and iii) rolling from preform, respectively. The wedge tools used in the analysed cases of CWR are shown in Figure 3.

The tool used in standard CWR, which is shown in Fig. 3a, was designed in compliance with the applicable rules. In this process, the central region of the billet is deformed by a wedge characterised by a forming angle of α=15° and a spreading angle of β=16.2°. It is worth stressing the fact that the β angle is greater than its maximum value (15°) recommended in the literature [1]. Nevertheless, the product of the tangents of the selected angles α and β is equal to 0.0778 and is lower than the critical value of 0.08. Two short guides hold the billet in a fixed position early in the rolling process as the wedge cuts into the material. The ends of the workpiece are deformed by the wedges described by angles α=20° and β=12°, the values of which are within the range recommended for CWR. The wedges cut into the workpiece after deforming its centre. On their side the wedge tools have 150 mm long recesses for mounting the side cutters for cutting off excess material. The tool used in wasteless rolling, which is shown in Fig. 3b, has the same wedges

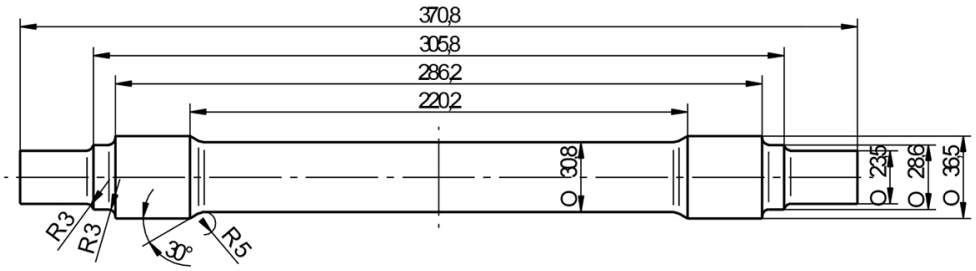

Fig. 1. Railcar axle rolled in a scale of 1:6 (dimensions in the figure are given for hot forming conditions)

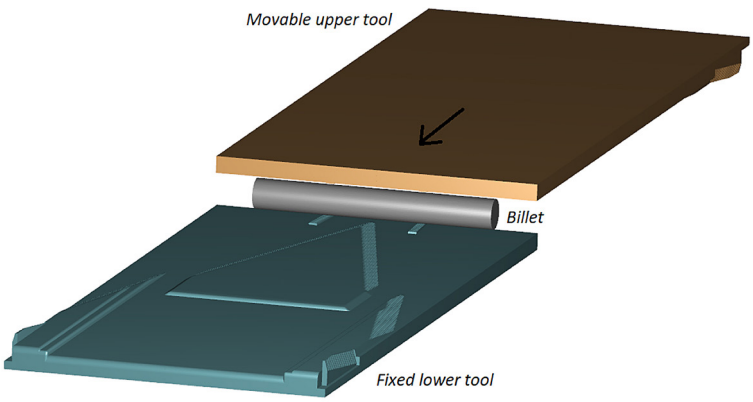

Fig. 2. Geometric model of one of the analyzed CWR cases for the axles of railway wagons

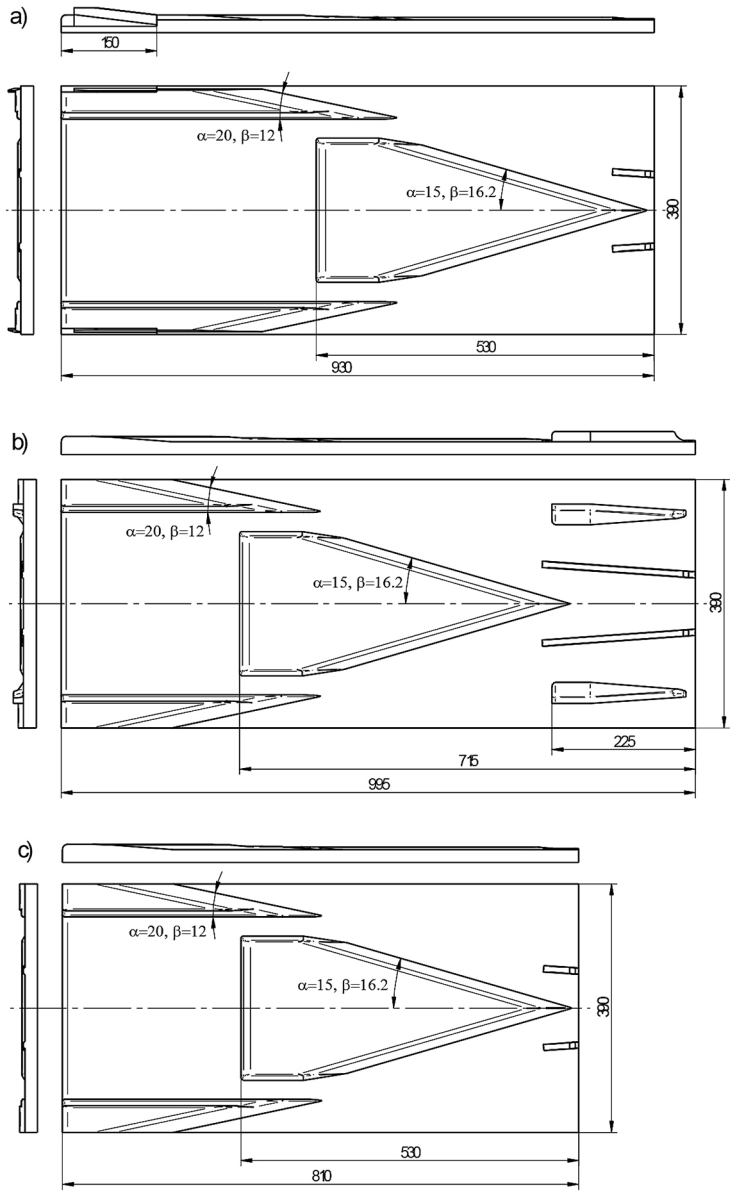

Fig. 3. Tools used in the numerical calculations of: (a) standard rolling, (b) wasteless rolling, (c) rolling from preform

as the standard rolling tool but has no side cutters. However, the tool is provided with two additional wedges for shaping tapered ends on the billet. These wedges are mounted at the very tip of the tool, which made it necessary to increase the length of the guideways for keeping the billet in stable location at the beginning of the rolling process. As a result of this modification, the tool is longer (by 7%) than that used in standard rolling. Fig. 3c illustrates the wedge tool employed in the CWR process in which a railcar axle was rolled from a preform. The design of this tool is the same as that of the tool used in standard CWR yet it has no side cutters. It must however be remembered that this case of CWR requires performing an additional forging operation to shape billet ends. The above-mentioned cases of CWR were compared via numerical simulations performed using the Forge® software. The billets for rolling were made of the 42CrMo4 grade steel and had a diameter of 36.5 mm and a length of 290 mm (in standard CWR) and 272 mm (in the other two cases of CWR). The rheology of 42CrMo4 steel is described by the Hansel-Spittel constitutive law:

$$\sigma_f = 1872.07 \cdot e^{-0.0029T} \cdot \varepsilon^{-0.1123} \cdot \dot{\varepsilon}^{0.1437} \cdot e^{-0.0488/\varepsilon} \quad (1)$$

where: σ – the flow stress, T – the temperature, ε – the strain, $\dot{\varepsilon}$ – the strain rate.

The calculation assumes that the billet is a viscoplastic object, while the tools are rigid objects. billet was discretized using 3D P1+ tetrahedral linear elements with a bubble node. The average element size was 1.75 mm for the billet. The above dimensions applied to hot forming conditions. The temperature of the billet was set to 1150°C, and the temperature of the tools was 50°C. The heat transfer coefficient between the workpiece and the tools was set equal to 10 kW/m^{2}K. The friction at the billet - tool interface was determined using the Tresca model expressed by the following relation:

$$\tau = m \cdot k \tag{2}$$

where: τ – the shear stress on contact surface, k – the pure shear yield stress ($k=\sigma_f/\sqrt{3}$), and m – the friction factor. The friction factor for the hot rolling process is assumed to be $m = 0.8$.

NUMERICAL RESULTS

First of all, the three selected cases of rolling were analysed in terms of their stability and workpiece shape changes. Figure 4 shows the changes in the shape of a workpiece during standard rolling. In the first stage of CWR, the tools deform the central region of the workpiece. When the workpiece centre undergoes sizing, the side wedges cut into the workpiece and begin to deform its ends. Once the side wedges have cut into the workpiece to the maximum depth, the workpiece centre is no longer in contact with the tools, which is desired because this eliminates all rolling motion resistances in this region of the workpiece. Following the sizing of the workpiece ends, the waste material on the ends is cut off and a finished railcar axle is obtained. Figure 5 shows the changes in the shape of a workpiece during wasteless rolling. At the beginning of the rolling process, the additional wedges shape the tapered ends of the workpiece. After that, the workpiece is formed into a railcar axle in the same way as in standard CWR. Completion of the rolling process involves sizing the ends of the workpiece. The last of the considered cases of CWR requires the use of a preform with appropriately profiled ends. These can be shaped in different ways, e.g. a tapered end is shaped on a press in two press strokes (see Fig. 6). The workpiece is rotated by an angle of 90°

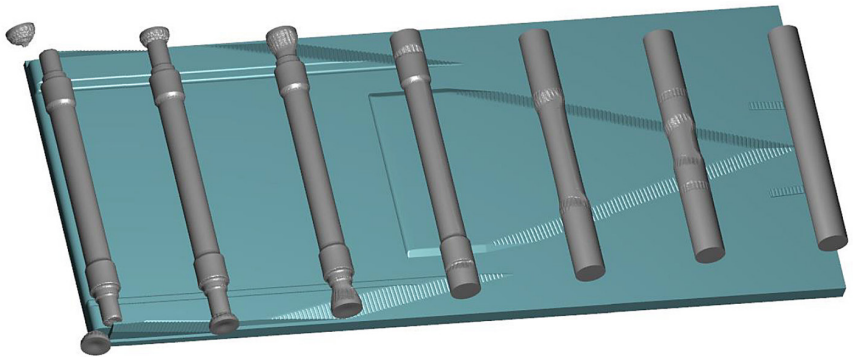

Fig. 4. Workpiece shape changes during standard rolling

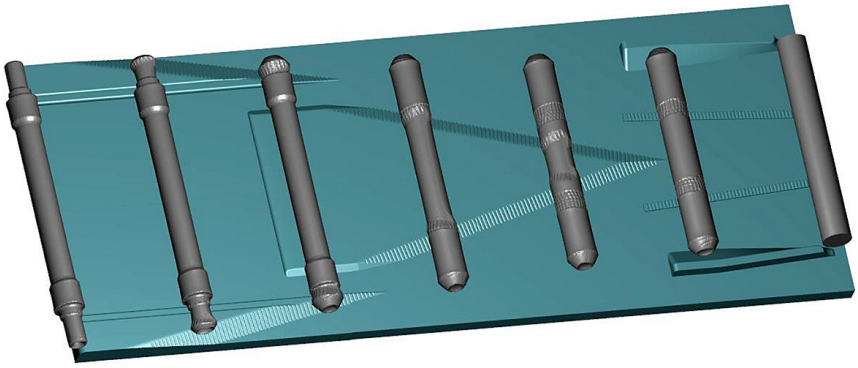

Fig. 5. Progression in shape of a workpiece during wasteless rolling of a railcar axle from a cylindrical billet

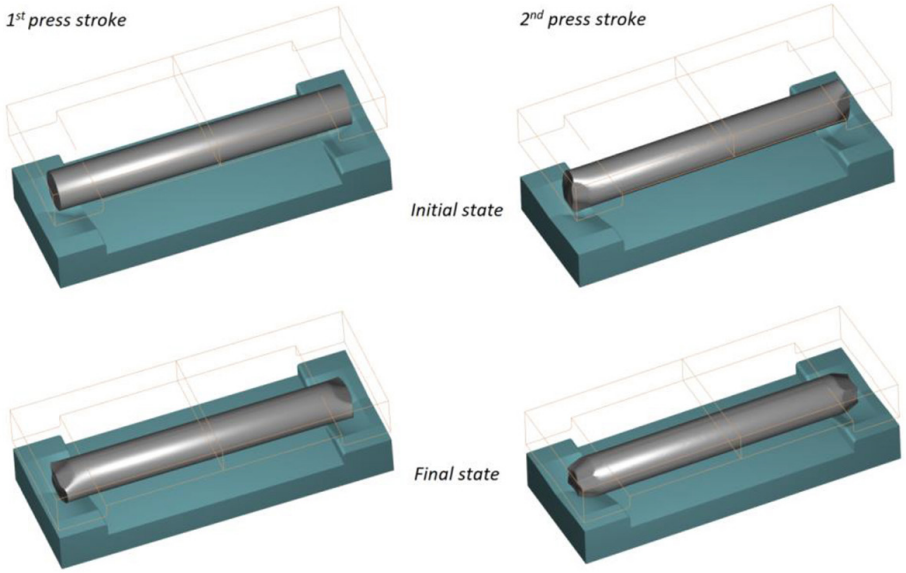

Fig. 6. Stages in hydraulic press forging of workpiece ends

between the press strokes. As a result of forging, the obtained tapered end is completely concavity-free. The preform is then subjected to rolling (Fig. 7), and the rolling process is conducted in the same way as in standard CWR (without cutting off the defective ends). The axes obtained from all the CWR cases analysed have the required geometry and are free of externally occurring faults. Nevertheless, as shown in Fig. 8, only the axle produced by standard CWR has flat surface ends. In the other two cases, this surface is concave. Nevertheless, the concavity depth is not considerable, and the concavity can be removed by machining. The mass of waste in the case of standard rolling was 0.2 kg and in the other two cases just 0.05 kg.

A serious failure mode occurring in CWR of railcar axles is the creation of cracks along the central zone of the workpiece [22, 37]. The likelihood of fracture formation is predicted based on damage function distributions which are shown for the analysed cases in Fig. 9. The distributions were determined using the normalized Cockcroft-Latham criterion. For fracture to have occurred, the value of the damage function needs to be greater than the breakpoint value of the critical damage. The billets for rolling were made of steel grade 42CrMo4. The critical damage value for this steel grade determined via rotary compression test [38] is 2.8 at 1150 °C. Such high damage values were not observed in any of the analysed cases of CWR (see Fig. 9). It was also found that the probability of crack formation (at the bottom of the end concavity) was the highest in wasteless rolling, where the maximum value of the damage function was only slightly lower than the critical damage value.

Force and energy parameters are an important aspect of CWR process design. Figure 11 shows the transverse loads achieved for the analysed example of CWR. This load causes elastic deflection

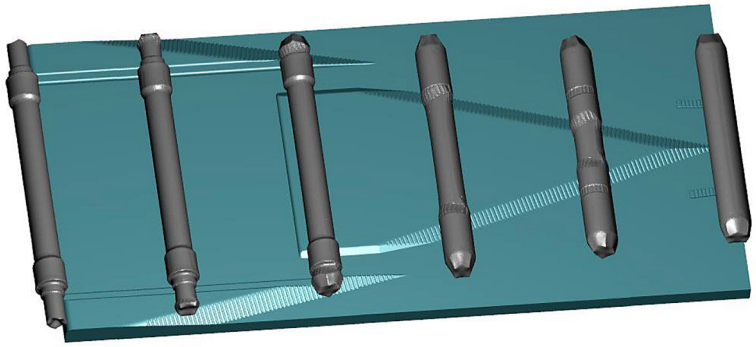

Fig. 7. Geometric progression of a workpiece during wasteless rolling of a railcar axle from a preform

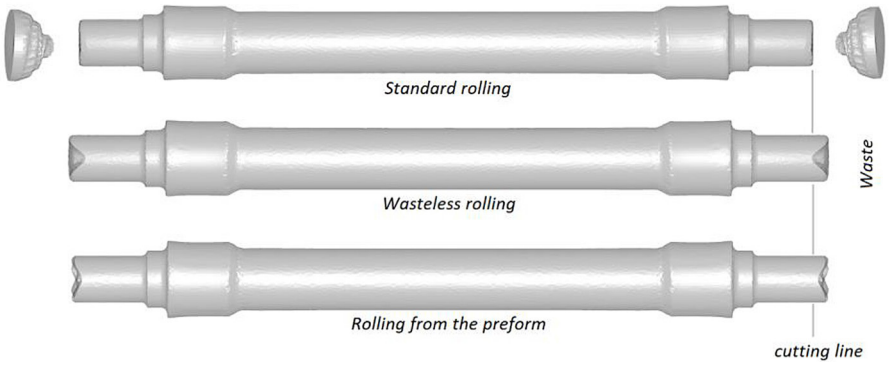

Fig. 8. Railcar axles achieved in the analysed example of CWR

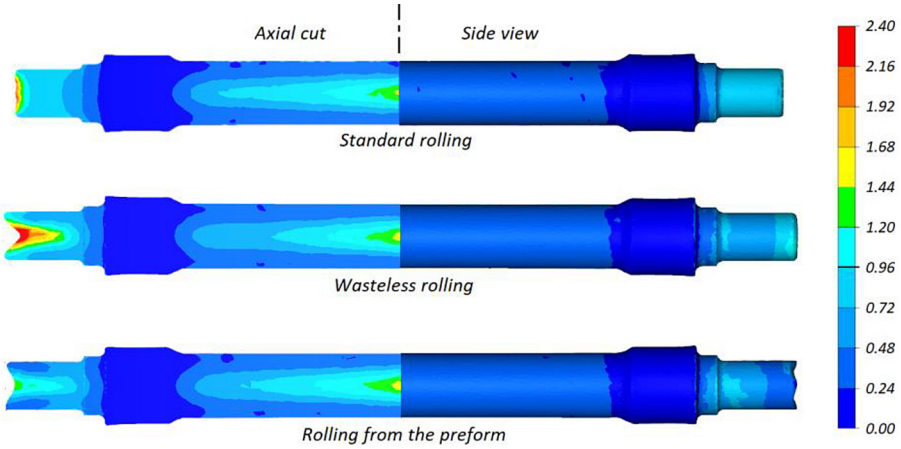

Fig. 9. Damage function values in railcar axles produced by analysed CWR processes

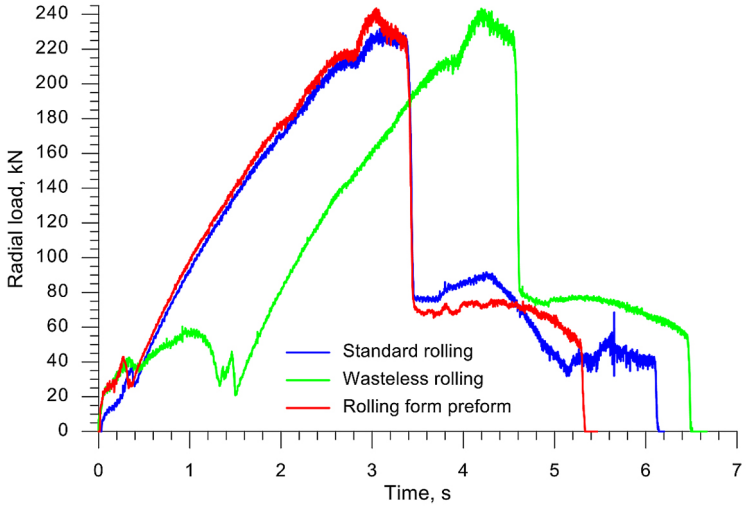

Fig. 10. Radial loads in the analysed cases of CWR

of the mill frame, which affects the diameter accuracy of rolled parts. As shown in Figure 11, the highest values are observable in the final stage when the workpiece centre is deformed. Also, among the analyses cases of CWR, the radial load is the lowest in standard rolling. Nevertheless, the differences between the maximum values are insignificant and do not exceed 5%, which has practically no impact on the stability of the rolling process. Even smaller differences can be observed between the maximum forming loads (acting on the wedge), the distributions of which

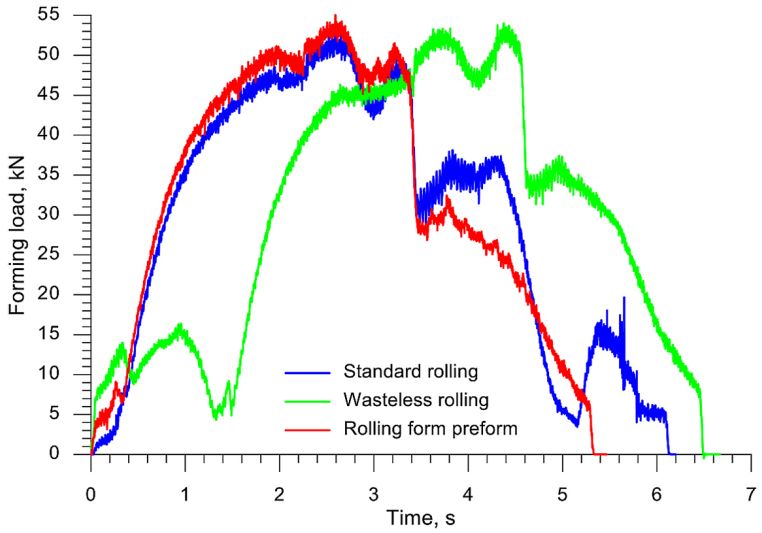

Fig. 11. Forming (tangential) loads in the analysed CWR processes

are shown in Figure 11. For this case, the difference between the loads is only 2%. The obtained forming load distributions can be used to calculate the theoretical work that is required to roll an axle. The lowest value of this work (52.64 kJ) was observed in rolling from a preform because an additional operation had to be performed to shape tapered ends on the workpiece. The highest work value was observed in wasteless rolling and equalled 58.43 kJ (which amounts to 111% of the work value in CWR from preform). In standard CWR the work is 54.35 kJ (which amounts to 103.6% of the work value in CWR from preform). One can observe a close relationship between tool length (Fig. 3) and work. Increasing the length of the tool results in an increase in the value of the work.

Summing up the numerical results, it can be concluded that the standard CWR process is the most material-consuming (material consumption was 6.6% greater than in the two other processes). Also, the axle ends formed by standard CWR have the highest surface quality. To achieve a similar end face quality in wasteless rolling and rolling from a preform, an additional operation must be performed to cut off the incorrect tips of the workpiece (according to the cutting line marked in Fig. 8). The transverse force is the lowest in standard CWR. It should also be stressed that wasteless CWR requires the use of the longest tools and the greatest work to produce an axle, whereas in rolling from a preform an additional operation must be performed to form tapered ends on the workpiece. Taking the above into consideration, the standard CWR process was selected for further experimental verification.

EXPERIMENTS

Validations were conducted on a hydraulic drive rolling mill with flat wedge accessed at the Lublin University of Technology. The wedge tools described by the parameters specified in Fig. 3a were fabricated using a CNC milling machine. Serrations (Fig. 12) were made on the forming faces (side walls) of the tools in order to minimize the risk of uncontrolled slip that would stop rotation of the workpiece. The tools were attached to the fixed lower plate and to the mill slide.

Fig. 12. Wedge tool used in experiments

Rods with a 36 mm diameter and 286 mm length were applied as the billets for experimental tests. They were heated to a temperature of 1170 °C in an electrical chamber furnace. After heating, they were put on the guideways of the fixed lower tool. Next, the mill slide was started and moved with a velocity of v=300 mm/s. An axle was formed by rolling the workpiece over the fixed lower tool. In the end stage of the rolling tests, the lateral knives cut off the defective workpiece ends with concavities. The above CWR system for manufacturing railway axles is shown in Fig. 13. The temperature used for heating the billet was 20 °C higher than that applied in the numerical simulation. This resulted from the fact that prior to rolling it was necessary to perform operations that caused material cooling but were not included in the numerical simulation (these operations included transferring the billet from the furnace, scale removal, putting the billet on the lower tool). As a result, the temperature distribution of the billet was close to the temperature distribution applied in the numerical simulation, as proved by the thermogram in Fig. 14. The temperature of the material decreased during rolling because the heat was carried away to the tools and environment. In spite of this fact, the temperature of the billet remained within the hot forming conditions for the 42CrMo4 grade steel. Figure 15 shows examples of railway axles of 1:6 scale that were rolled at the Lublin University of Technology. The axles are free from surface defects (e.g. overlap) and have the desired shape and dimensions. As far as rolling accuracy is concerned, their diameters are within a tolerance range of $d_{+0.2}^{+1.2}$. The positive dimensional deviations are due to cross-sectional ovalisation resulting from the application of high values of the β angle and relatively short sizing zones. It must also be stressed that the manufacturing quality of the produced axles is satisfactory. To determine whether the use of standard CWR would lead to voids formation in central part of the axis, one of the axles was subjected to destructive testing. A milling operation was performed to expose a longitudinal plane going through the axle's axis of rotation (Fig. 16). Macroscopic examination clearly

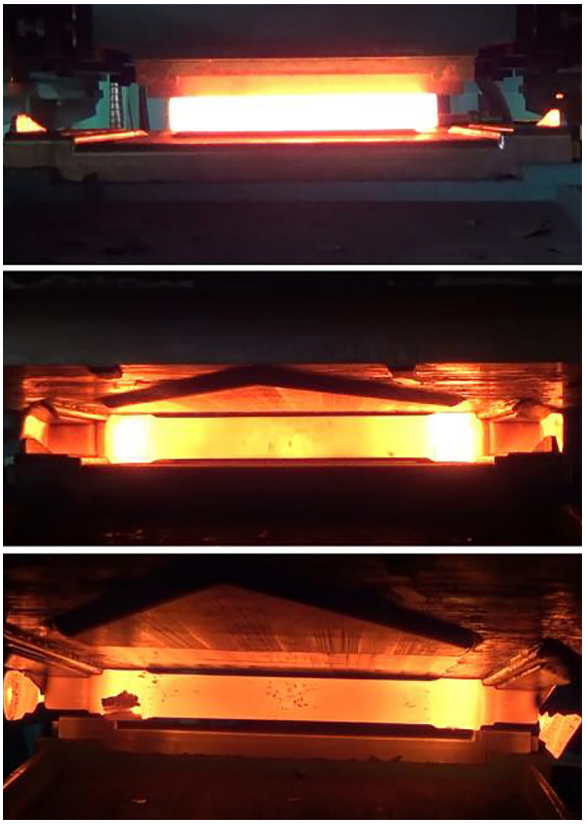

Fig. 13. CWR of a railcar axle conducted under laboratory conditions at the Lublin University of Technology

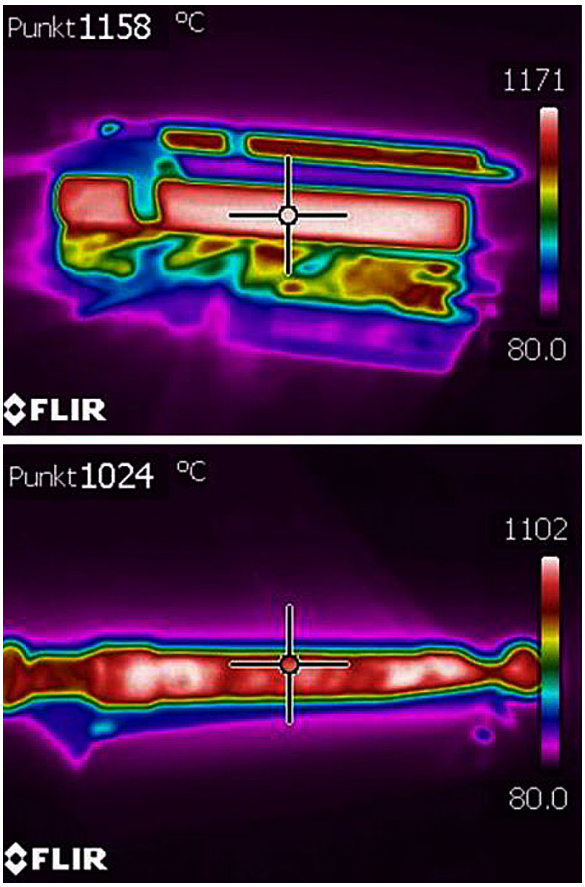

Fig. 14. Temperature measurement in a billet and in a railcar axle during experiments

Fig. 15. Railcar axles rolled in 1:6 scale at the Lublin University of Technology

Fig. 16. Axial section of a rolled axle

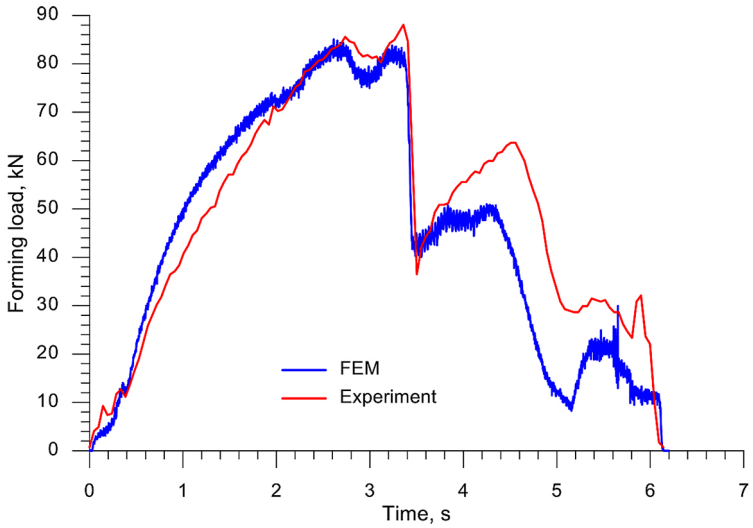

Fig. 17. Comparison of the experimental and numerical forming loads

showed that the axle manufactured by the selected CWR system was devoid of voids and cracks.

Figure 17 shows a comparison of the experimental and numerical forming loads in the analysed CWR process. The numerical load value was calculated by summing up the forming loads (Fig. 10) and 15% of the radial load value (Fig. 11). The other component of the forming load (which was determined empirically) compensated the resistances to motion which occurred in the flat wedge mill used in the experiments. The comparison demonstrates that the experimental and numerical loads are almost identical in terms of quality. It should be added that the loads are considerably higher when the central region of the workpiece was deformed rather than in the stage of forming the workpiece ends, which undoubtedly results from differences in the length of these workpiece regions. The maximum experimental load was 88.06 kN, and this value was higher by 3.5% than the numerical load which amounted to 85.5 kN. Greater discrepancies between the experimental and numerical forming loads were observed in the second stadium of the CWR process, i.e. during the formation of

the billet tips. The fact that the experimental loads were higher probably resulted from increased cross-sectional ovalisation due to mill stretch. The obtained loads were used to determine the value of work that was necessary to produce an axle. It was 91.75 kJ and 83.42 kJ in the experiment and numerical simulation, respectively. Therefore, the calculation error for work was 9.1%. Summing up the numerical and experimental results, it can be concluded that the developed numerical model of the CWR process accurately reproduced the real process conditions.

CONCLUSIONS

Three cases of the CWR process for producing a railcar axle were analysed numerically: standard rolling, wasteless rolling and rolling from a preform. The numerical results lead to the following conclusions:

- All analysed cases of CWR produce railcar axles with the desired shape; the produced axles are free from defects;
- The standard CWR process is more material-consuming than the other two methods, but it does not require performing an additional operation to cut off the defective ends of the workpiece;
- Wasteless CWR is the least energy consuming process, but it requires the use of a billet with profiled ends, e.g. by an additional forging operation;
- Standard CWR is characterized by the lowest forming loads, with their values being several percent lower than those obtained in the other two cases of CWR. Considering the above numerical results, the standard CWR process was selected for further laboratory tests. The railcar axle obtained from the experiments (in a scale of 1:6) had the required shape and dimensions; it was also free from any internal or external defects.

Acknowledgment

The research was financed in the framework of the project: Development of new rolling technologies for rail axle forgings, No. LIDER/9/0060/L-12/20/NCBR/2021. Total cost of the Project: 1 466 831.25 PLN. The project is financed by the National Centre for Research and Development under the 12th edition of the LIDER Programme.

REFERENCES

1. Pater Z. Cross-Wedge Rolling. In: Comprehensive Materials Processing; S.T. Button, Ed.; Elsevier Ltd. 2014; 3: 211-279.
2. Bulzak T., Pater Z., Tomczak J., Majerski K. Hot and warm cross-wedge rolling of ball pins – Comparative analysis. Journal of Manufacturing Processes 2020; 50: 90-101.
3. Ghiotti A., Fanini S., Bruschi S., Bariani P.F. Modelling of the Mannesmann effect. CIRP Annals - Manufacturing Technology 2009; 58: 255-258.
4. Pater Z., Tomczak J., Bulzak T., Li Z. Analysis of the use of variable angular parameter tools in cross-wedge rolling. Journal of Manufacturing Processes 2022; 83: 768-786.
5. Bulzak T., Pater Z., Tomczak J. Validation of a new system for measuring material constants representing damage limits. Measurement 2022; 196: 111265.
6. Wei X. H., Shu X. D. Study on production mechanism of end concavity in cross wedge rolling. Advanced Materials Research 2011; 314-316: 468-472.
7. Guo D., Lu X. Effect of process parameters on the volume of the stub bar of Rolled Pieceby Cross Wedge Rolling under the different end shapes. Journal of Engineering Mechanics and Machinery 2017; 2(1): 1-7.
8. Sun B. S., Zhao Z. L., Wang C. W. Effect of process parameters on the end-face quality of cross-wedge rolling (CWR) shaft from titanium alloy Ti6Al4V. Metalurgija 2019; 58(1-2): 127-130.
9. Pater Z, Tomczak J, Bulzak T. Cavity formation in cross-wedge rolling processes. Journal of Iron and Steel Research International 2019; 26(1): 1-10.
10. Shu X. D., Wei X. H., Chen L. P. Influence analysis of block wedge on rolled-piece end quality in cross wedge rolling. Applied Mechanics and Materials 2011; 101-102: 1055-1058.
11. Pater Z., Tomczak J., Bulzak T. New forming possibilities in cross wedge rolling processes. Archives of Civil and Mechanical Engineering 2018; 18(1): 149-161.
12. Wei J., Shu X., Tian D., et al. Study in shaft end forming quality of closed-open cross wedge rolling shaft using a wedge block. International Journal of Advanced Manufacturing Technology 2017; 93(1-4): 1095-1105.
13. Shu X. D., Wei J., Liu C. Study on the control of end quality by one closed cross wedge rolling based wedge block. Metalurgija 2017; 56: 123-126.
14. Zeng J., Xu C.., Ren W., Li P. Study on the deformation mechanism for forming shafts without concavity during the near-net forming cross wedge rolling process. International Journal of Advanced Manufacturing Technology 2017; 91(1-4): 127-136.
15. Yang C., Zheng Z., Hu Z. Simulation and experimental study on the concavity of workpiece formed by cross wedge rolling without stub bar. International

Journal of Advanced Manufacturing Technology 2018; 95(1-4): 707-717.

16. Han S., Shu X., Chen T., et al. Study on the progressive forming mechanism of multi-step shafts based on convex-end billet in the cross wedge rolling technology. Journal of Mechanical Science and Technology 2019; 33(12): 6021-6035.
17. Wang R., Wang Y., Wang H., Chen J. Y., Shu X. D. Study on roll-cutting forming method of conical end blank for cross wedge rolling (CWR) without stub bar. Metalurgija 2020; 59(1): 18-22.
18. Gronostajski Z., Pater Z., Madej L., Gontarz A., Lisiecki L., Łukaszek-Sołek A. Recent development trends in metal forming. Archives of Civil and Mechanical Engineering. 2019; 19(3): 898-941.
19. Pater Z., Bulzak T., Tomczak J. Numerical simulation of a cross-wedge rolling process in a mill with horizontally stacked rolls. Mechanik. 2022; (5-6): 54-58.
20. Sun B. S., Zeng X. L., Shu X. D., Peng W. F., Sun P. Feasibility study on forming hollow axle with multi-wedge synchrostep by cross wedge rolling. Applied Mechanics and Materials 2012; 201-202: 673-677.
21. Peng W., Zheng S., Chiu Y., Shu X., Zhan L. Multi-wedge cross wedge rolling process of 42CrMo4 large and Long Hollow shaft. Rare Metal Materials and Engineering 2016; 45(4): 836-842.
22. Bulzak T. Ductile fracture prediction in cross-wedge rolling of rail axles. Materials 2021; 14(21) :6638.
23. Piedrahita F., Aranda L. G., Chastel Y. Three dimensional numerical simulation of cross-wedge rolling of bars. In: Proc. of the 8th International Conference on Technology of Plasticity ICTP, Verona, Italy 2005, 257-258.
24. Silva M. L. N., Pires G. H., Button S. T. Damage evolution during cross wedge rolling of steel DIN 38MnSiVS5. Procedia Engineering 2011; 10: 752-757.
25. Kache H., Stonis M., Behrens B. A. Development of a warm cross wedge rolling process using FEA and downsized experimental trials. Production Engineering 2012; 6(4-5): 339-348.
26. Meyer M., Stonis M., Behrens B. A. Cross wedge rolling and bi-directional forging of preforms for crankshafts. Production Engineering 2015; 9(1): 61-71.
27. Meyer M., Stonis M., Behrens B. A. Cross wedge rolling of preforms for crankshafts. Key Engineering Materials 2012; 504-506: 205-210.
28. Behrens B. A., Stonis M., Rasche N. Influence of the forming angle in cross wedge rolling on the multi-directional forging of crankshafts. International Journal of Material Forming 2018; 11(1): 31-41.
29. Pérez I., Ambrosio C. Material saving by means of CWR technology using optimization techniques. AIP Conference Proceedings 2017; 1896: 190001.
30. Gutierrez C., Langlois L., Baudouin C., Bigot R., Fremeaux E. Impact of tool wear on cross wedge rolling process stability and on product quality. AIP Conference Proceedings 2017; 1896: 190008.
31. Pater Z., Tomczak J., Bulzak T. Fem simulation of the cross-wedge rolling process for a stepped shaft. Strength of Materials 2017; 49(4): 521-530.
32. Pater Z., Tomczak J., Bulzak T. An innovative method for forming balls by cross rolling. Materials 2018; 11(10): 1793.
33. Pater Z, Tomczak J. A new cross wedge rolling process for producing rail axles. MATEC Web of Conferences 2018; 190: 11006.
34. Pater Z. Study of cross wedge rolling process of BA3002-type railway axle. Advances in Science and Technology Research Journal 2022; 16(2): 225-231.
35. Kruse J., Jagodzinski A., Langner J., Stonis M., Behrens B. A. Investigation of the joining zone displacement of cross-wedge rolled serially arranged hybrid parts. International Journal of Material Forming 2020; 13(4): 577-589.
36. Pater Z., Tomczak J., Bulzak T. Walczuk-Gągała P. Novel damage calibration test based on cross-wedge rolling. Journal of Materials Research and Technology 2021; 13: 2016-2025.
37. Bulzak T., Pater Z., Tomczak J., Wójcik Ł., Murillo-Marrodán A. Internal crack formation in cross wedge rolling: Fundamentals and rolling methods. Journal of Materials Processing Technology 2022; 307: 117681.
38. Pater Z., Tomczak J., Bulzak T., Wójcik Ł. Conception of a three roll cross rolling process of hollow rail axles. ISIJ International 2021; 61(3): 895-901.